Electronic Supplementary Information for "Ultrafast Coherent Vibrational Dynamics in Dimethyl Methylphosphonate Radical Cation"

Derrick Ampadu Boateng[a], Gennady L. Gutsev[b], Puru Jena[c], and Katharine Moore Tibbetts[a]

[a]Department of Chemistry, Virginia Commonwealth University, Richmond, VA 23284, USA

[b] Department of Physics, Florida A&M University, Tallahassee, FL 32307, USA

[c]Department of Physics, Virginia Commonwealth University, Richmond, VA 23284, USA

SI Measurement of Pulse Duration (FROG)

A home-built Frequency Resolved Optical Gating (FROG) setup was used to measure the spectrograms for each pulse and the time-dependent electric fields were retrieved with an open-source MATLAB code[1] based on the retrieval algorithm in Ref.[2]. Figure S1 shows the spectrograms (top panels) and retrieved temporal electric fields (bottom panels) for the 800 nm, 1200 nm, and 1500 nm pump pulses, as well as the 800 nm probe pulse. The time-dependent intensity is shown in blue and the temporal phase shown in red. The retrieved FWHM pulse durations are indicated in each panel.

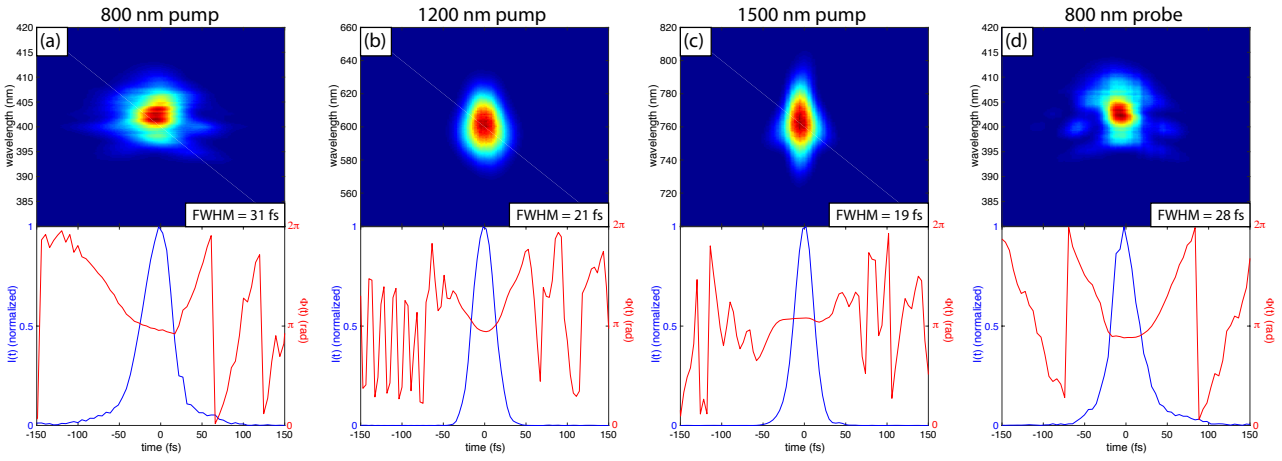

Figure S1: Two-dimensional spectrograms recorded with SHG-FROG setup (top panels) and retrieved time-dependent electric fields (bottom panels).

SII Xe^+ Cross-Correlation Measurements

In order to both verify the pulse duration and identify the zero delay position of the stage, the vacuum chamber was filled with Xe gas and pump-probe measurements taken using 6×10^{13} W cm^{-2} pump pulses at 800 and 1500 nm and 1×10^{13} W cm^{-2} probe pulses at 800 nm. The transient Xe^+ signals are shown in Figure S2.

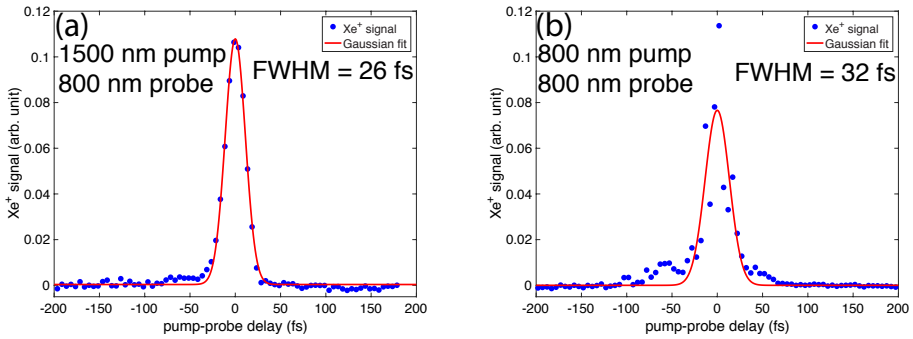

Figure S2: Cross-correlation measurements of Xe^+ signal taken with (a) 1500 nm pump - 800 nm probe, and (b) 800 nm pump - 800 nm probe. Gaussian fits to the experimental data and extracted FWHM values are shown.

SIII Additional pump-probe measurements

A 1600 nm pump pulse was also tested to assess the hypothesis that adiabatic ionization is needed to effectively prepare the coherent state in $DMMP^+$ because the pulse duration of the 1600 nm pulse from the OPA increases to 28 fs due to the limited phase matching bandwidth (Figure S3(a)-(b)). Large oscillation amplitudes in the yields of $DMMP^+$ and its dissociation products are observed (Figure S3(c)). Additional pump and probe energies were tested with the 800 nm pump setup in order to determine the combination of pump and probe energies that produces the largest amplitude oscillations. Decreasing the energy of either pump or probe only decreased the oscillation amplitude (Figure S4).

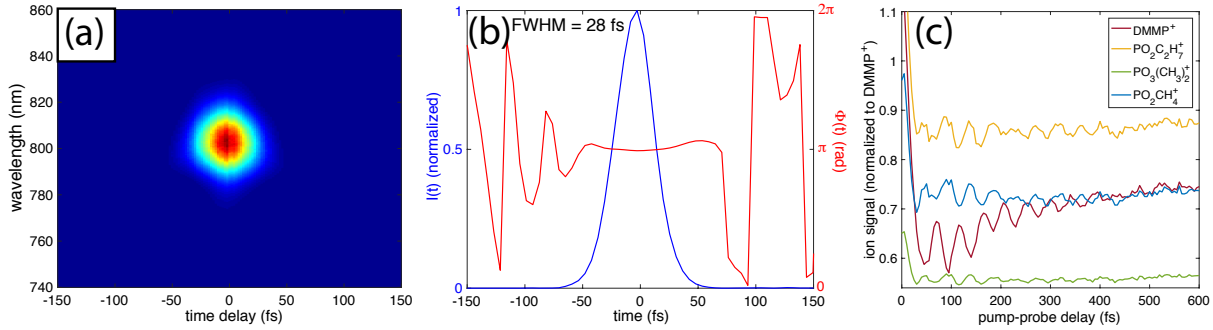

Figure S3: (a) FROG spectrogram of 1600 nm pump. (b) Retrieved electric field. (c) Transient ion signals of $DMMP^+$ and dissociation products with 1600 nm pump.

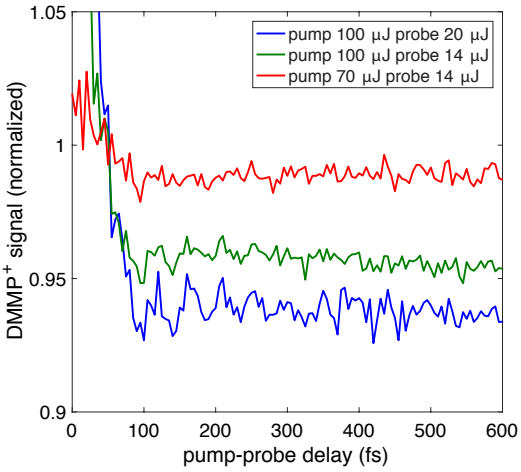

Figure S4: Transient ion signals of $DMMP^+$ at various pump and probe energies for 800 nm pump. Signals are normalized to the yield at negative time delays.

SIV Results of calculations

Table S1 reports the calculated normal modes of $DMMP^+$ at the BPW91 and B3LYP levels. Both the harmonic and anharmonic frequencies are shown. The coherently excited normal mode is highlighted in red. Table S2 reports the differences in bond lengths and bond angles between the optimized neutral and cation geometries of DMMP. The atom labels are given in Figure S5. All radii R(x,y) are given in Angstroms and all angles A(x,y,z) are given in degrees. The two coordinates contributing to the coherently excited normal mode are highlighted in red.

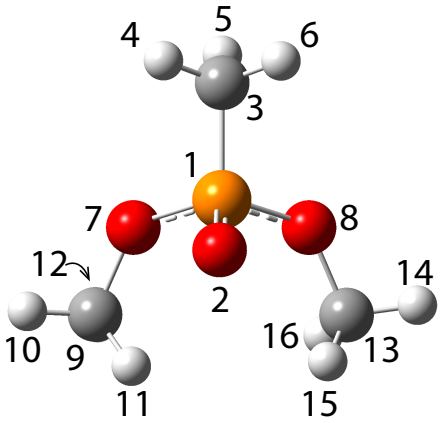

Figure S5: DMMP structure with atoms labeled according to the labels in Table S2.

BPW91 mode	ν_{harm} (cm^{-1})	ν_{anharm} (cm^{-1})	I_{harm} km/mol	I_{anharm} km/mol	**B3LYP**	ν_{harm} (cm^{-1})	ν_{anharm} (cm^{-1})	I_{harm} km/mol	I_{anharm} km/mol
1	40.91	61.33	1.69	1.58		19.27	-467.96	0.001	221.11
2	80.87	43.91	1.70	1.16		69.54	-119.57	0.23	3.69
3	97.04	63.32	1.23	0.58		84.03	74.78	2.96	2.19
4	120.73	94.20	1.48	2.73		99.72	83.09	2.46	4.50
5	151.96	121.67	2.03	6.14		133.60	160.11	4.54	9.09
6	161.71	147.04	6.31	27.54		154.69	135.60	0.77	11.28
7	166.71	152.59	14.69	13.58		166.52	159.89	15.15	16.07
8	232.45	230.90	7.77	13.63		204.71	218.16	10.28	4.58
9	236.88	217.98	4.38	11.21		253.09	245.36	3.46	2.54
10	270.05	257.44	1.63	34.61		271.82	268.02	8.01	6.20
11	270.43	260.17	4.85	5.21		346.10	331.31	10.01	3.79
12	456.72	444.07	33.44	34.79		471.50	462.55	26.80	25.72
13	610.71	583.28	4.86	2.59		659.12	641.83	24.98	23.41
14	686.55	649.17	0.41	0.85		760.83	715.42	0.64	0.92
15	772.79	754.66	17.55	15.98		766.97	742.20	4.70	8.98
16	863.04	827.65	6.71	49.04		864.02	834.09	13.13	6.70
17	863.82	832.65	9.71	97.59		934.66	910.52	15.19	8.37
18	913.70	898.08	22.36	16.42		952.94	935.45	34.93	28.81
19	946.88	916.91	5.08	11.09		1044.26	1005.66	180.21	88.76
20	1036.50	1009.49	249.38	65.55		1065.54	1026.02	371.47	310.84
21	1105.33	1075.83	14.25	0.97		1165.06	1136.55	2.74	1.53
22	1112.65	1079.99	2.44	4.54		1168.16	1137.93	0.20	0.72
23	1138.09	1112.54	3.31	20.37		1193.50	1156.89	31.98	6.54
24	1138.17	1114.13	7.49	6.20		1193.89	1159.18	17.05	6.04
25	1325.94	1293.71	32.06	26.55		1375.94	1345.20	32.59	28.91
26	1400.74	1353.62	7.30	11.82		1454.26	1417.39	17.40	18.97
27	1403.29	1359.26	2.28	55.20		1454.42	1417.39	10.49	11.43
28	1409.46	1365.70	24.75	35.02		1476.73	1440.99	3.58	1145.53
29	1411.58	1371.51	32.34	22.24		1478.22	1442.73	4.47	5.19
30	1414.79	1376.17	12.53	6.19		1481.76	1433.39	13.10	198.80
31	1415.36	1375.39	9.75	12.14		1491.56	1443.71	0.64	6.07
32	1443.52	1402.71	106.92	90.26		1502.53	1450.00	7.20	6.83
33	1460.52	1411.80	72.77	51.57		1507.95	1455.68	59.09	28.08
34	2978.86	2854.75	74.53	354.81		3059.30	2942.92	16.93	19.38
35	2981.99	2850.16	21.29	671.12		3078.34	2980.18	0.53	5.50
36	3002.87	2880.43	16.53	18.41		3079.80	2976.54	7.36	4.70
37	3073.87	2899.24	5.61	27.73		3149.72	3005.34	6.74	5.21
38	3074.81	2909.01	6.22	19.48		3150.15	3005.92	5.39	4.33
39	3096.35	2947.64	6.79	5.58		3176.98	3036.45	2.61	2.40
40	3099.79	2952.78	6.10	4.72		3177.53	3034.16	2.66	3.88
41	3113.58	2937.77	17.65	26.30		3201.86	3056.59	1.45	1.31
42	3114.85	2941.32	13.77	20.43		3202.33	3057.00	0.65	0.26

Table S1: Calculated normal modes of $DMMP^{+}$.

	BPW91			B3LYP		
coordinate	neutral	cation	% diff.	neutral	cation	% diff.
R(1,2)	1.497	1.540	2.811	1.484	1.582	6.555
R(1,3)	1.813	1.783	1.622	1.804	1.775	1.591
R(1,7)	1.646	1.614	1.950	1.627	1.565	3.836
R(1,8)	1.630	1.615	0.932	1.611	1.570	2.551
R(3,4)	1.097	1.097	0.073	1.090	1.091	0.110
R(3,5)	1.098	1.097	0.073	1.091	1.091	0.046
R(3,6)	1.098	1.098	0.027	1.091	1.092	0.018
R(7,9)	1.445	1.457	0.851	1.438	1.471	2.274
R(8,13)	1.446	1.457	0.754	1.438	1.469	2.148
R(9,10)	1.097	1.095	0.246	1.090	1.088	0.183
R(9,11)	1.096	1.100	0.347	1.089	1.088	0.046
R(9,12)	1.101	1.096	0.427	1.093	1.085	0.741
R(13,14)	1.099	1.100	0.091	1.092	1.088	0.339
R(13,15)	1.099	1.095	0.346	1.091	1.088	0.312
R(13,16)	1.095	1.096	0.064	1.088	1.086	0.211
A(2,1,3)	116.55	119.49	2.527	116.46	116.31	0.132
A(2,1,7)	113.69	108.27	4.766	113.29	106.83	5.697
A(2,1,8)	117.33	108.11	7.858	116.85	103.78	11.189
A(3,1,7)	106.01	104.50	1.431	106.09	106.80	0.666
A(3,1,8)	100.04	104.49	4.442	100.71	106.90	6.143
A(7,1,8)	101.16	111.98	10.701	101.57	116.65	14.851
A(1,3,4)	110.75	110.51	0.215	110.71	109.84	0.791
A(1,3,5)	109.25	108.64	0.551	109.31	109.01	0.271
A(1,3,6)	108.83	108.63	0.183	109.02	109.02	0.003
A(4,3,5)	109.66	109.80	0.129	109.56	109.74	0.163
A(4,3,6)	109.58	109.79	0.193	109.52	109.53	0.005
A(5,3,6)	108.74	109.44	0.638	108.69	109.69	0.922
A(1,7,9)	120.04	129.32	7.732	121.29	131.30	8.249
A(1,8,13)	119.42	129.34	8.307	120.70	131.79	9.192
A(7,9,10)	110.97	111.81	0.757	110.81	110.24	0.508
A(7,9,11)	106.27	106.32	0.757	106.41	17.60	1.112
A(7,9,12)	110.38	106.12	3.860	110.30	105.20	4.624
A(10,9,11)	110.20	111.46	1.646	110.28	111.85	1.429
A(10,9,12)	109.66	111.46	1.646	109.64	110.90	1.150
A(11,9,12)	109.31	109.18	0.118	109.35	110.78	1.312
A(8,13,14)	110.36	106.25	3.721	110.25	106.35	3.536
A(8,13,15)	110.73	111.85	1.006	110.57	110.84	0.247
A(8,13,16)	105.97	106.16	0.174	106.20	105.90	0.283
A(14,13,16)	110.13	111.68	1.407	110.12	111.69	0.990
A(14,13,16)	109.69	109.14	0.499	109.70	110.79	0.990
A(15,13,16)	109.87	111.47	1.455	109.93	111.02	0.928

Table S2: Coordinate differences.

SV Curve fitting results

Table S3 presents the fitting coefficients to Eq. S.1

$$S(\tau) = ae^{-\tau/T}\left[\sin\left(\frac{2\pi}{t}\tau + \phi\right) + b\right] + c, \tag{S.1}$$

where the curves are reported in the main text, Figure 3. The reported errors in the table denote 95% confidence intervals. The R^2 values for each fit are also given.

ion	λ (nm)	a	T (fs)	t (fs)	ϕ (rad)	b	c	R^2
$DMMP^+$	800	0.019 ± 0.008	180 ± 10	45.8 ± 0.8	4.2 ± 0.5	0.3 ± 0.2	0.937 ± 0.002	0.51
	1200	0.072 ± 0.007	150 ± 10	45.3 ± 0.3	4.1 ± 0.2	-2.5 ± 0.2	0.780 ± 0.002	0.98
	1500	0.100 ± 0.009	150 ± 10	45.0 ± 0.6	4.1 ± 0.1	-1.8 ± 0.1	0.805 ± 0.002	0.98
$PO_2C_2H_7^+$	1200	0.033 ± 0.009	130 ± 30	45.7 ± 0.9	1.4 ± 0.4	-1.3 ± 0.3	1.113 ± 0.001	0.81
	1500	0.043 ± 0.009	150 ± 30	45.1 ± 0.4	1.4 ± 0.2	-0.2 ± 0.1	1.06 ± 0.001	0.81
$PO_3(CH_3)_2^+$	1200	0.007 ± 0.002	230 ± 60	45.9 ± 0.9	1.3 ± 0.5	-4 ± 1	0.374 ± 0.002	0.86
	1500	0.014 ± 0.004	170 ± 50	45.5 ± 0.6	1.1 ± 0.3	-0.5 ± 0.2	0.329 ± 0.001	0.72
$PO_2CH_4^+$	1200	0.018 ± 0.006	230 ± 70	45.0 ± 0.7	0.6 ± 0.4	-1.9 ± 0.6	0.931 ± 0.003	0.77
	1500	0.04 ± 0.01	140 ± 40	45.2 ± 0.7	0.9 ± 0.3	0.4 ± 0.2	0.823 ± 0.001	0.70

Table S3: Curve fitting coefficients for all transient ions.

References

[1] S. Byrnes and A. Wyatt, *Frequency Resolved Optical Gating*, MATLAB File Exchange. Last accessed October 13, 2017.

[2] D. J. Kane, *IEEE J. Quant. Electron.*, 1999, **35**, 421–431.